Decontamination of Radionuclides from Concrete by Microwave Heating. I: Theory

Zdeněk P. Bažant, F.ASCE,[1] and Goangseup Zi[2]

Abstract: The paper analyzes a proposed scheme of decontamination of radionuclides from concrete structures, in which rapid microwave heating is used to spall off a thin contaminated surface layer. The analysis is split in two parts: (1) the hygrothermal part of the problem, which consists in calculating the evolution of the temperature and pore pressure fields, and (2) the fracturing part, which consists in predicting the stresses, deformations and fracturing. The former is assumed to be independent of the latter, but the latter is coupled to the former. The heat and moisture transfer governing the temperature and pore pressure fields induced by the decontamination process is analyzed using an improved form of Bažant and Thonguthai's model for heat and moisture transfer in concrete at high temperatures. The rate of the distributed source of heat due to the interaction of microwaves with the water contained in concrete is calculated on the basis of the standing wave normally incident to the concrete wall. Since the microwave time period is much shorter than the time a heating front takes to propagate over the length of microwave, and since concrete is heterogeneous, the ohmic power dissipation rate is averaged over both the time period and the wavelength. The reinforcing bars parallel to the surface are treated as a smeared steel layer. The recently developed microplane model M4 serves as the constitutive model for nonlinear deformation and distributed fracturing of concrete. Application of the present model in numerical computations is relegated to a companion paper which follows.

DOI: 10.1061/(ASCE)0733-9399(2003)129:7(777)

CE Database subject headings: Concrete; Microwaves; Contamination; Contaminants; Heating; Diffusion; Thermal stresses; Pore pressure.

Introduction

Concrete is ubiquitous in nuclear facilities. As a consequence of their longtime operation, various radionuclides, such as strontium, cesium, cobalt, uranium, etc. (Spalding 2000), have gradually diffused from the environment into a surface layer of concrete. Although the radionuclide concentrations are very small, the exposure to radiation over many years could be hazardous to human health. Typically, the contaminated layer is only 1–10 mm thick [Fig. 1(a)] (White et al. 1995), and so a demolition of the whole structures is unnecessary. Nevertheless, to guarantee a safe longtime work environment, the contaminated layer needs to be removed and properly disposed of as nuclear waste.

Possible decontamination techniques include removal of the contaminated layer by hammer and chisel, by high-pressure water jet, and by various thermal treatments. This paper deals with the last, which can be of two types: (1) heat conduction from a heated surface, and (2) heating generated by microwaves throughout the volume of concrete. The former type has been studied for a long time with regard to fire resistance of buildings, and even more deeply with regard to the effects of hypothetical nuclear reactor accidents (e.g., Bažant and Thonguthai 1978, 1979; Ahmed and Hurst 1997; Gawin et al. 1999). As a result, the material characteristics needed to calculate the temperatures and pore pressures due to heat conduction from a heated surface are known relatively well (Harmathy 1970; Harmathy and Allen 1973; Bažant and Kaplan 1996; Neville 1997; Vodák et al. 1997).

The recent studies of the decontamination process have emphasized microwave heating, which allows a much faster removal of the contaminated layer (within only about 10 s; White et al. 1995). The driving force of the spalling is the microwave heat source which is distributed through the volume of concrete and is generated by microwaves emitted from a powerful applicator [Fig. 1(a)].

Microwave heating has already been applied in various civil engineering problems. For instance, (1) microwaves have been extensively used for nondestructive evaluation of materials. (2) Microwave ovens (instead of the traditional ovens) have been used for effective drying of porous geomaterials (Wei et al. 1985). (3) Microwave heating has been used to accelerate the curing process of concrete at early ages (Watson 1968a; Moukwa et al. 1991). (4) Microwaves of low frequency and low power density were shown capable of heating properly insulated concrete specimens to an almost uniform temperature (Hertz 1981, 1983), which made it possible to measure the effect of temperature on compression strength in the absence of temperature gradients. (5) Microwaves of high frequency, which are suitable for the present decontamination process, have been shown capable of generating a localized field of high stress that can serve as a demolition tool (Watson 1968b; Wace et al. 1989; White et al. 1995).

Some valuable investigations of the microwave decontamination of concrete have already been undertaken. Li et al. (1993)

[1]McCormick School Professor and W. P. Murphy Professor of Civil Engineering and Materials Science, Northwestern Univ., 2145 Sheridan Rd., Evanston, IL 60208. E-mail: z-bazant@northwestern.edu

[2]Research Associate, Dept. of Civil Engineering, Northwestern Univ., 2145 Sheridan Rd., Evanston, IL 60208. E-mail: g-zi@northwestern.edu

Note. Associate Editor: Franz-Josef Ulm. Discussion open until December 1, 2003. Separate discussions must be submitted for individual papers. To extend the closing date by one month, a written request must be filed with the ASCE Managing Editor. The manuscript for this paper was submitted for review and possible publication on March 12, 2002; approved on October 29, 2002. This paper is part of the ***Journal of Engineering Mechanics***, Vol. 129, No. 7, July 1, 2003. ©ASCE, ISSN 0733-9399/2003/7-777–784/$18.00.

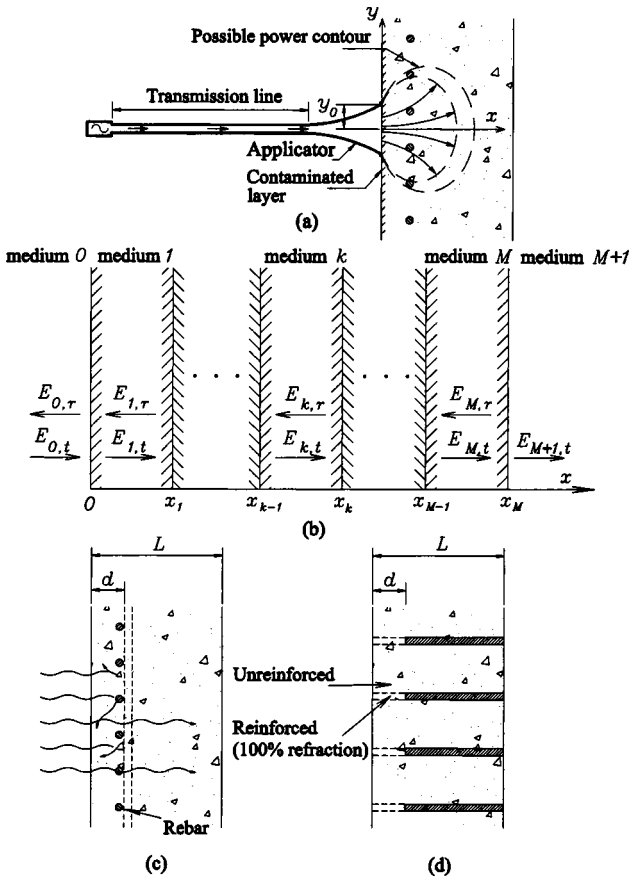

Fig. 1. (a) Sketch of microwave power decontamination system; (b) transmission (t) and reflection (r) of transmission electron microscopy wave at interfaces of different media; (c) typical layout of concrete wall and wave reflection by reinforcing bars and aggregates; and (d) partition of concrete body into reinforced segments and unreinforced segments

analyzed one-dimensional temperature profiles using a linear heat transfer model. Lagos et al. (1995) extended the heat transfer model to two dimensions and calculated the heat generation rate based on the standing wave normally incident to a homogeneous concrete wall. They smeared the reinforcing bars into an infinitely thin layer whose reflection factor was determined according to the area–ratio of the bars. They assumed the dielectric properties of concrete to be constant over the thickness of concrete during the decontamination process. However, they could not study the development of pore pressures because they did not model the moisture transfer coupled to the heat transfer. They assumed the surface layer to spall off when the compressive stress in the direction parallel to surface under a perfect restraint in that direction exhausts the compressive strength of the concrete. They did not take into account the deformation of the body surrounding the heated zone.

The practical objective of this study, which was summarized at a recent conference (Bažant and Zi 2001), is twofold: (1) to present a model-based mathematical analysis of microwave heating and spalling of concrete; and (2) to apply it to the decontamination process that takes into account not only the thermal deformation and surface layer restraint but also the moisture transfer, pore pressures, and overall deformation of the structure. The theory will be explained in this paper, while the companion paper that follows (Zi and Bažant 2003) will present the numerical application. The constitutive, fracture, thermal, and diffusion models of concrete applied here are of course known. Nevertheless, since these models exist in different variants, and since some minor modifications were made in them in this project, they are briefly described in the Appendices of parts I and II of this study.

Heat Generation by Transverse Electromagnetic Waves

The microwaves represent electromagnetic waves of frequency 300 MHz–30 GHz. The energy carried by electromagnetic waves through surface S is

$$-\int_S \mathcal{P}\cdot d\mathbf{S} = -\int_S \mathbf{E}\times\mathbf{H}\cdot d\mathbf{S} = \frac{\partial}{\partial t}\int_V (w_e + w_m)dV + \int_V p_\sigma dV. \tag{1}$$

(e.g., Cheng 1983) where $\mathcal{P}$ = Poynting vector characterizing the power density of the electromagnetic wave, $\mathbf{E}$ = electric field strength vector; $\mathbf{H}$ = magnetic field strength vector; $d\mathbf{S} = \mathbf{n}dS$, where $d\mathbf{S}$ = surface element and $\mathbf{n}$ = its unit normal; V = volume of body; $\epsilon = \epsilon' - i\epsilon''$ = complex dielectric permittivity; $\mu = \mu' - i\mu''$ = complex magnetic permittivity; $\sigma = \omega\epsilon''$ = dielectric conductivity; $\omega = 2\pi f$ = angular velocity; f = frequency, $w_e = \varepsilon E^2/2$ = electric energy density; $w_m = \mu H^2/2$ = magnetic energy density; $p_\sigma = \sigma E^2$ = ohmic power dissipation; t = time; and V = volume.

Because the heat generation rate is a function of the electric field strength, one needs to solve the electric field strength vector $\mathbf{E}$ to obtain the heat source. On exit from the microwave applicator, the waves are guided and simple. But farther away the electromagnetic field can become complicated [Fig. 1(a)]. An accurate solution would have to be obtained numerically from the Maxwell equations, which is not a simple affair. For our purpose, however, an approximate solution can be obtained by using the solution of a standing electromagnetic wave, particularly the solution of a transverse electromagnetic wave normally incident to a half space of a dielectric material, the concrete. The heat source calculated in this manner needs of course some further adjustment to obtain the proper power distribution (Thuéry 1992).

Electric Strength of Standing Electromagnetic Waves

Let us now review the solution of the transverse electromagnetic waves, which form a standing wave pattern. The propagation of electromagnetic waves is governed by the Maxwell equations in which the electric field strength and magnetic field strength are coupled. Because the concentration of dielectric sources due to ferromagnetic materials in concrete is usually negligible (Li et al. 1993), the electromagnetic wave generation inside concrete may be neglected, which means that the Maxwell equations become decoupled (von Hippel 1954);

$$\nabla^2\mathbf{E} = \epsilon\mu\frac{\partial^2\mathbf{E}}{\partial t^2} \tag{2a}$$

and

$$\nabla^2\mathbf{H} = \epsilon\mu\frac{\partial^2\mathbf{H}}{\partial t^2} \tag{2b}$$

The transverse electromagnetic waves may be considered to be parallel, and their incidence to the concrete surface to be normal.

Therefore, aside from time t, the dielectric field depends only on coordinate x normal to the surface [Fig. 1(b)]. Eqs. (2*a*) and (2*b*) are simply solved as

$$\mathbf{E}=\mathbf{E}_0 e^{i\omega t-\gamma x} \tag{3a}$$

and

$$\mathbf{H}=\mathbf{H}_0 e^{i\omega t-\gamma x} \tag{3b}$$

where γ = complex propagation factor.

At the interface of two different media, the electromagnetic wave is partially reflected and partially transmitted as a refracted wave. The magnitude of refracted wave is given by Fresnel's equation, and the reflection and refraction angles by Snell's law (e.g., von Hippel 1954). If the wave is incident to the interface of two dielectric media in normal direction, the wave forms a standing wave pattern. Since only a normal incidence is considered here, the wave can be calculated simply from the continuity condition at each interface (e.g., Cheng 1983; Wait 1985).

Consider the concrete wall, sketched in Fig. 1(b), to be subdivided into parallel strips normal to the surface which either contain steel reinforcement or not [Fig. 1(d)]. Medium 0 represents air and media $k=1,2,\cdots M$ the layers of concrete with different water contents [Fig. 1(b)]. Medium $M+1$ represents air in the case of unreinforced strips, or steel in the case of reinforced strips in Fig. 1(d). By analogy with the transmission line theory (which is used to calculate the voltage and current in an electric circuit), the wave solutions in medium k are obtained as follows (Wait 1985):

$$E(x)=C_k(e^{-\gamma_k x}+R_k e^{\gamma_k x})$$

and

$$H(k)=(C_k/\eta_k)(e^{-\gamma_k x}-R_k e^{\gamma_k x}) \quad \text{for } 0<x<l \tag{4}$$

where C_k = transmission factor; R_k = reflection factor; and η_k = intrinsic impedance of medium k. Here $\eta_k=\gamma_k/i\omega\epsilon_k=\sqrt{\mu_k/\epsilon_k}$. The transmission factor of air is given as the initial electric strength E_0. The reflection factor between air and the first concrete layer is denoted as R_0

$$R_0=(Z_1-\eta_0)/(Z_1+\eta_0) \tag{5}$$

where Z_1 = transmission impedance of medium 1. The impedance of medium k is obtained from the transmission line theory as

$$Z_k=\eta_k(Z_{k+1}+\eta_k \tanh\gamma_k l_k)/(\eta_k+Z_{k+1}\tanh\gamma_k l_k) \tag{6}$$

$$Z_{M+1}=\eta_k(\eta_{M+1}+\eta_M \tanh\gamma_M l_M)/(\eta_M+\eta_{M+1}\tanh\gamma_M l_M) \tag{7}$$

where $l_k=x_k-x_{k-1}$ = width of each layer. For unreinforced strips, $\eta_{M+1}=\eta_0$. For reinforced strips, $\eta_{M+1}=0$, which implies an almost 100% reflection by reinforcing bars. From the condition of continuity at each interface, R_k and C_k are obtained as follows:

$$R_k=e^{-2\gamma_k x_{k-1}}[E_{k-1}(x_{k-1})-H_{k-1}(x_{k-1})\eta_k]/[E_{k-1}(x_{k-1})+H_{k-1}(x_{k-1})\eta_k] \tag{8}$$

$$C_k=[E_{k-1}(x_{k-1})]/[e^{-\gamma_k x_{k-1}}+R_k e^{\gamma_k x_{k-1}}] \tag{9}$$

As we have seen, the solution of the electric field strength E_k of medium k [Fig. 1(b) [Fig. 1(b), Eq. (4)] is a complex function. The real part of E_k is taken as the actual solution. The rate of volumetric heat generation by the transverse electromagnetic waves can be obtained from Eq. (1). Because the wave period $T=1/f$ is far shorter than the time that the thermal heat front takes to advance through one wavelength of the electromagnetic wave, it is meaningful to average the heat generation rate over period T;

$$I_{(h)}^{\text{ave}}=\frac{1}{T}\int_0^{T=2\pi/\omega}\sigma[\text{Re}(E)]^2 dt \tag{10}$$

$$=\frac{1}{2}\sigma\|C\|^2\{e^{-2\alpha x}+\|R\|^2 e^{2\alpha x}+[R'\cos 2\beta x-R''\sin 2\beta x]\} \tag{11}$$

where $C=C'+iC''$ = transmission factor; $R=R'+iR''$ = reflection factor; β = phase factor; and α = attenuation factor ($1/\alpha$ represents the depth through which the field strength decays to $1/e=0.368$ of its original value); here $\gamma=\sqrt{i\mu\omega(\sigma+i\epsilon\omega)}=\alpha+i\beta$ = complex propagation factor.

A typical layout of a reinforced concrete wall is depicted in Fig. 1(c). The wave is reflected and scattered by steel reinforcing bars as well as the aggregates. Although the arrangement of the bars is three dimensional, they may be approximately treated one dimensionally and thus their location will be characterized just by the depth d below the surface (Fig. 1). Therefore, due to the heterogeneity of concrete wall, we may take the spatial average of Eq. (11) over the wave number $2\pi/\beta$. As a result, the averaged heat generation rate is obtained as

$$I_{(h)}=\tfrac{1}{2}\sigma\|C\|^2(e^{-2\alpha x}+\|R\|^2 e^{2\alpha x}) \tag{12}$$

Note that, when the second term, which represents power reflection by rebars, is neglected, Eq. (13) becomes the well-known Lambert's law:

$$I_{\text{Lambert}}=I_0 e^{-2\alpha x} \tag{13}$$

where I_0 = heat generation rate at the surface. The advantage of Lambert's law, which is widely used in low-temperature food engineering (Metaxas and Meredith 1983; Taoukis et al. 1987; Meredith 1998), is that it is simple and easy to understand.

Effect of Reinforcing Bars on Microwave Penetration

As an approximation, the reinforced concrete may be considered for our purposes as a parallel combination of unreinforced and reinforced strips in the direction normal to surface, labeled by subscripts U and R; Fig. 1(d). The overall average volumetric heat generation in the reinforced concrete wall can be obtained as the average of the heat generations in two adjacent strips

$$I_{(h)}=\begin{cases}(1-p)I_U+pI_R & \text{for } x<d\\ (1-p)I_U & \text{for } x\geq d\end{cases} \tag{14}$$

where p = area fraction of the steel reinforcing bars on a plane parallel to concrete surface; and I_U, I_R = rate of heat generation in unreinforced and reinforced strips normal to surface, respectively. Both I_U and I_R are obtained from Eq. (13). Note that, because of different boundary conditions, the electric strength of E_U is different from E_R; it is assumed that E_U is transmitted into air at the opposite surface of the wall, and E_R is perfectly reflected at the location of the steel bars d.

For the sake of simplicity, the foregoing analysis neglects calculation of the three-dimensional diffraction and scattering of the electromagnetic waves due to steel bars. The diffraction and scattering are surely much less significant than the wave reflection, because of the steep power decay in the concrete cover (see Part II).

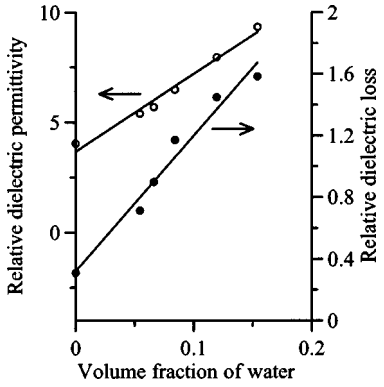

Fig. 2. Relative dielectric properties of concrete depending on water content (Hasted and Shah 1964)

Dielectric Properties of Concrete

The properties of dielectric materials generally depend on moisture contents and temperature changes (Metaxas and Meredith 1983). The relative dielectric permittivity $\kappa' = \varepsilon'/\varepsilon_0$ and the relative dielectric loss $\kappa'' = \varepsilon''/\varepsilon_0$ of concrete quadratically increase as a function of volume fraction of water v_w (Hasted and Shah 1964; Shah et al. 1965) (ε_0 = dielectric permittivity of air = 8.86×10^{-12} F/m). The dielectric constants κ' and κ'' change significantly when v_w exceeds about 20%. When v_w is less than 20%, the changes can be approximated by linear functions (Fig. 2). The concretes that need to be decontaminated are usually old concretes, in which the volume fraction of water is around 7%. Because the water content is a function of pore pressure and temperature, as described by the constitutive laws [Eq. (17)], the dielectric properties of concrete depend not only on the water content but also, indirectly, on temperature. Regarding a direct effect of temperature on the dielectric properties, no information is available and probably this effect is negligible.

Application of Microplane Constitutive Model M4

To determine whether a given microwave source will achieve spalling and predict the depth of spalling, a good constitutive model relating the stress and strain in concrete is needed. Li et al. (1993) considered a restrained one-dimensional elastic bar and estimated its stress simply as $\sigma = -E\alpha\Delta T$. This estimate, however, ignores the nonlinearity of deformation on approach to spalling and the confining effect of the body surrounding a hot spot heated by microwaves. A three-dimensional constitutive model needs to be used.

For this purpose, version M4 of the microplane model (briefly described in Appendix III of Part II) has been adopted (Bažant et al. 2000b; Caner and Bažant 2000). The microplane model is a powerful explicit model that yields the best data fit over broad range of nonlinear triaxial behavior, softening damage and tensile cracking of concrete (Bažant et al. 2000b; Caner and Bažant 2000). Fracture propagation can be handled with model M4 most easily in the sense of the crack band model.

The microplane model differs from the classical tensorial models based on plasticity by the fact that the constitutive law is expressed in terms of vectors rather than tensors. The vectors are the stress and strain vectors on planes of all possible orientations within the material. Thanks to all possible microplane orientations, the model automatically satisfies tensorial invariance conditions. The strain vectors on the microplanes are assumed to be the projections of the continuum strain tensor, and the stress tensor is related to the microplane stress vectors through a variational principle. For a detailed description of the microplane model and the history of development, with a literature review, see Bažant et al. (2000b), and for various related aspects also Brocca and Bažant (2000).

Thermal Degradation of Concrete

Besides the triaxial and strain softening behavior, concrete also undergoes thermal degradation and transient creep. Both the compressive strength f_c and the Young's modulus E degrade as the temperature increases. The degradation is typically determined from tests of the residual mechanical properties of concrete exposed for some time [typically 12 h, (Felicetti and Gambarova 1998)] to various controlled temperature histories. The surface temperature, as calculated in Part II of this study (Zi and Bažant 2003), reaches less than 400°C during the 10 s of heating envisaged for decontamination. If this temperature were sustained for many hours, the compressive strength of concrete would degrade to about 85% of the original value (Bažant and Chern 1987). But what if this temperature lasts for only 10 s?

The degradation is caused by dehydration of the calcium silicate hydrates in cement paste. Since the chemical reactions of dehydration at high temperature cannot happen instantly and probably take much longer than the desired 10 s duration of the decontamination process, the degradation will be neglected.

The temperature increase near 400°C will intensify creep as well as the apparent effect of strain rate on the elastic modulus of concrete. This could be taken into account by introducing on the microplanes a creep law based on the Maxwell or Kelvin chain (Zi and Bažant 2001). According to finite element simulations, the maximum strain rate in the heated concrete prior to spalling, which occurs near the surface, is about $\dot{\varepsilon} = 1 \times 10^{-4}\ \mathrm{s}^{-1}$. Compared to the typical loading rate in quasi-static laboratory tests, which is about $5 \times 10^{-6}\ \mathrm{s}^{-1}$, the rate effect would increase the apparent Young's modulus to approximately 120% (Bažant et al. 2000a) of the normal value, but only near the place of maximum strain rate. Elsewhere the rate effect will be significantly less. The rate effect will be neglected in the present finite element computations.

It might seem that the rate effect might get offset somewhat by the effect of thermal degradation. However, thermal degradation is a far slower process (Ulm et al. 1999), which is surely negligible within the duration of 10 s.

Hygrothermal Strain

The thermal expansion coefficient α_T of cement mortar changes significantly with temperature, which is caused by moisture effects. But for concrete, the change of α_T with temperature is much less pronounced. This is explained by the restraining effect of aggregates in concrete, which are usually very stable chemically (Harmathy 1970; Bažant and Kaplan 1996; Neville 1997). Therefore the thermal expansion coefficient α_T will simply be taken as constant ($\approx \alpha_T = 10.0 \times 10^{-6}\ \mathrm{K}^{-1}$) in the temperature range of the decontamination process. Thus the strain rate $\dot{\varepsilon}_T$ due to thermal dilatation is expressed as

$$\dot{\varepsilon}_T = \alpha_T \dot{T}$$

Regarding shrinkage, two kinds must be distinguished: (1) the average shrinkage of the cross section of a concrete member, which is not a constitutive property but a property of the whole cross section, with an inevitably complex mathematical description (Hansen and Almudaiheem 1987; ACI 1994; Bažant and Baweja 1995; Bažant and Baweja 2000); and (2) the shrinkage at a point of the continuum approximating concrete, which is a constitutive property. Unfortunately, the latter is next to impossible to measure directly (direct measurements have been made only on cement paste shells 0.75 mm in thickness, which is the maximum thickness needed to ensure that the humidity profile across the wall would remain almost uniform during a programmed linear decrease of environmental relative humidity at the rate 3%/h; Bažant and Najjar 1972).

Therefore the constitutive shrinkage of the material had to be inferred indirectly—by fitting the finite element solutions of test specimens to the measured deformations and adjusting the shrinkage model until a good fit is obtained (Bažant and Chern 1987; Bažant and Xi 1994; Bažant et al. 1997). The conclusion from these studies is very simple:

$$\dot{\varepsilon}_h = \kappa_s \dot{h}$$

where κ_s = shrinkage coefficient (taken as $\kappa = 0.5 \times 10^{-3}$, according to model B3; Bažant and Baweja 2000).

Conclusions

1. The paper presents a mathematical formulation for analyzing a proposed technique of decontamination of concrete walls from radionuclides residing in a thin surface layer, which is to be spalled off by rapid microwave heating. The formulation consists of (1) a model for heat generation in the bulk of concrete by microwave power dissipation; (2) a model for heat and moisture transfer with buildup of pore pressure; (3) a constitutive model for nonlinear triaxial behavior and fracturing of concrete; and (4) numerical solution.
2. The heat and moisture transfer is based on the model of Bažant and Thonguthai (1978), which is improved by introducing a more realistic rapid increase of the magnitude of the moisture permeability upon exceeding 100°C. An ohmic heat source term representing the rate of heat generation by microwaves is included in the formulation.
3. A simple analytical expression for the heat generation rate is developed. The heat generation rate caused by normally incident transmission electron microscopy waves is averaged over both the frequency and the wavelength. The microwave power reflection by steel reinforcing bars is taken into account in the resulting formula. The special case for no reinforcement agrees with the Lambert's law used in food engineering. The heat generation rates are determined separately for two kinds of strips normal to wall surface: one representing an unreinforced concrete and the other a concrete containing reinforcement bars at which the microwave is 100% reflected.
4. The recently developed version M4 of microplane model for concrete is adopted for the analysis of stresses and fracturing. Shrinkage and swelling due to changes in water content are taken into account, but creep is neglected because the duration of the spalling process is very short (only about 10 s).

Appendix: Heat and Moisture Transfer in Concrete

Governing Equations

The mass conservation equation and heat conservation equation are

$$\frac{\partial w}{\partial t} + \nabla \cdot \mathbf{J} = I_{(w)} \tag{15a}$$

and

$$\frac{\partial}{\partial t}(\rho C T) + \nabla \cdot \mathbf{q} = I_{(h)} \tag{15b}$$

Here ∇ = gradient operator; T = temperature; ρ = mass density of concrete; C = specific heat of concrete; w = specific water content; C_w = specific heat of water; $\mathbf{J}$ = water flux vector; $\mathbf{q}$ = conductive heat flux vector; $I_{(h)}$ = distributed source of heat; and $I_{(w)}$ = distributed source of water, due to release of chemically bound water (Bažant and Thonguthai 1978; Bažant and Kaplan 1996); subscripts (w) and (h) are labels for water and heat.

The heat capacity of oven dried concrete can be used for C since the latent heat due to heating induced chemical decomposition of hydrates in cement paste is relatively small, and negligible for concrete (Harmathy and Allen 1973), due to its large volume fraction of aggregates. Although the apparent heat capacity of concrete depends on the water content, the mass fraction of water is usually so small (less than 6% of total mass of concrete, even at saturation) that this dependence may be neglected, for simplicity (Bažant and Thonguthai 1978).

The water flux $\mathbf{J}$ and the heat flux $\mathbf{q}$ may be expressed in terms of the gradient of water content w and the gradient of temperature T, respectively

$$\mathbf{J} = -\frac{a}{g}\nabla P \tag{16a}$$

and

$$\mathbf{q} = -k \nabla T \tag{16b}$$

where a = permeability; g = gravity acceleration; P = pore pressure; and k = heat conductivity. Heat is also transferred by the movement of water inside of concrete, which is described by the convection term $\mathbf{q}_{cv} = C_w T \mathbf{J}$. In concrete, however, this term is negligible, because the diffusivity to pore water is about 3 orders of magnitude smaller than the heat diffusivity.

Equation of State of Pore Water

Except for temperatures above the critical point of water (374.15°C), one must distinguish the vapor from the liquid water in the pores of concrete. These two phases of water can be assumed to be locally always in thermodynamic equilibrium. Bažant and Thonguthai's (1978, 1979) model based on this hypothesis was shown to give acceptable match of the test data. Because of the complexity of the pore system, and especially the role of water adsorbed in the nanopores of hydrated cement paste, the formulation of the sorption isotherms of concrete, i.e., the curves of specific water content w versus relative humidity of water vapor in the pores, $h = P/P_s(T)$ [where $P_s(T)$ = saturation pore pressure at temperature T], must be semiempirical. The isotherms are described as

$$\frac{w}{c} = \left(\frac{w_1}{c} h\right)^{1/m(T)} \quad \text{for } h \leq 0.96 \tag{17a}$$

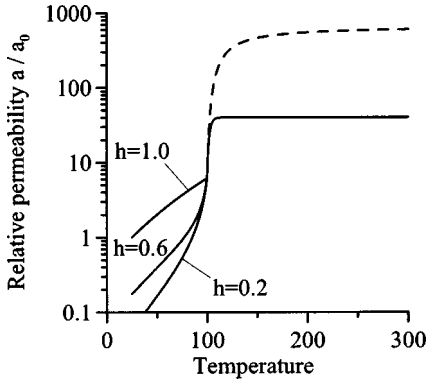

Fig. 3. Change of permeability by change of humidity and temperature

and

$$w=(1+3\varepsilon_V)n/v \quad \text{for} \quad h\geq 1.04 \tag{17b}$$

where T=temperature in °C; T_0=25°C; c=mass of anhydrous cement per unit volume of concrete; w_1=saturation water content at reference temperature T_0 (=25°C); $m(T)=1.04-[T'/(22.34+T')]$; $T'=(T+10)^2/(T_0+10)^2$; $d\varepsilon_V=d\sigma_V/(3K)+\alpha_T dT$; $\sigma_V=nP$; ε_V=linear volumetric strain; K=bulk modulus of concrete; n=porosity accessible to water; $v=v(T,P)$=specific volume of water; and α_T=coefficient of linear thermal dilatation of concrete. The porosity (pore volume accessible to water), which was estimated from considerations of weight loss, is expressed as $n=[n_0+\rho_0^{-1}w_d(T)]\psi(h)$ for $h\geq 1.04$, where n_0=reference porosity at 25°C; $w_d(T)$=weight loss [obtained from thermogravimetic measurements (Harmathy and Allen 1973)]; ρ_0=specific weight of water; and $\psi(h)=1+0.12(h-1.04)$.

Permeability and Conductivity

The permeability of concrete is a complex property. Because the capillaries in good quality concretes are not continuous, water molecules must pass through the nanopores in the hardened cement paste. Because the width of such pores (from 0.5 nm up) is much smaller than the mean free path of vapor molecules (about 80 nm at 25°C), water molecules cannot pass through the nanopores in a vapor state but must become adsorbed on the pore walls and migrate along adsorption layers. So the nanopores control the permeability, which explains the extremely low values of the permeability of concrete at normal temperatures. But this is not the case at high temperatures. When the temperature is increased above 100°C, the permeability jumps sharply up (Bažant and Thonguthai 1978). This can be explained by heat-induced changes in the structure of the smallest pores, particularly elimination of the narrowest necks, of nanometer dimensions, on the passages through cement paste. Based on data fitting, the permeability was inferred to jump up about 200×, but the present optimum fits of test data shown later indicates that the permeability jumps up, around 100°C, only about 6.5× (Fig. 3). The initial trend of function $f_3(T)$, which represents the permeability increase upon exceeding 100°C, is the same as proposed in Bažant and Thonguthai's (1978) work, but the magnitude of the jump needs to be scaled down, as represented by the following function:

$$a=a_0 f_1(h) f_2(T) \quad \text{for} \quad T\leq 100°\text{C} \tag{18a}$$

and

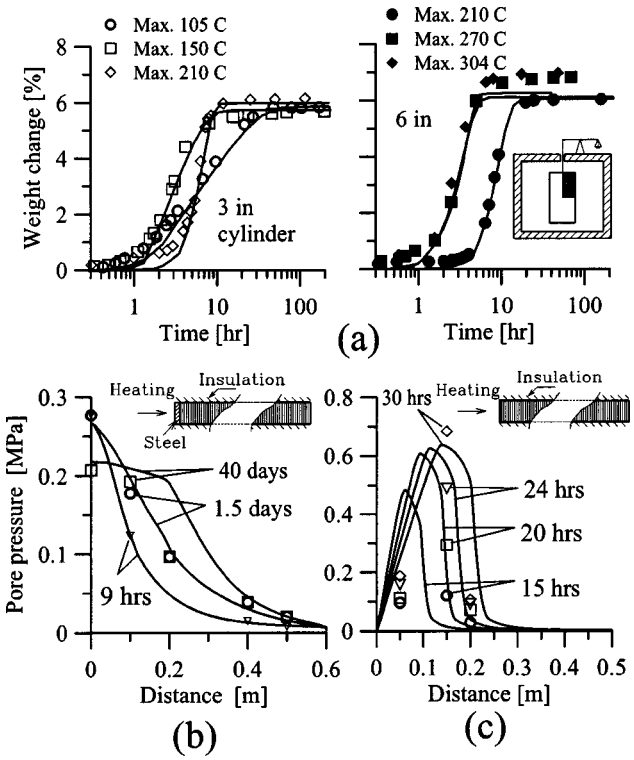

Fig. 4. Fits of (a) Bažant and Thonguthai's experiments (1978); (b) England and Ross' experiments (1970); and (c) by model proposed; symbols represent experimental data and solid lines represent fitting

$$a=a_0 f_2(100) f_3(T) \quad \text{for} \quad T>100 \tag{18b}$$

where a_0=reference permeability at 25°C. Function $f_1(h)$ characterizes the permeability corresponding to moisture transfer along the adsorbed water layers. The temperature dependence of permeability below 100°C is given by an Arrhenius-type equation $f_2(h)$;

$$f_1(h)=\alpha+\frac{1-\alpha}{1+\left(\frac{1-h}{1-h_c}\right)^4}, \quad \text{for} \quad h\leq 1; \quad f_1(h)=1, \quad \text{for} \quad h\geq 1 \tag{19}$$

$$f_2(T)=\exp\left[\frac{Q}{R}\left(\frac{1}{\overline{T}_0}-\frac{1}{\overline{T}}\right)\right] \tag{20}$$

where $\alpha=1/[1+0.253(100-\min(T,100°\text{C}))]$; $h_c=0.75$, $\overline{T}$=absolute temperature; Q=activation energy for water migration; and R=gas constant. Based on data fitting, the value $Q/R=2,700$ K was recommended (Bažant and Najjar 1972). Function $f_3(T)$, which describes the abrupt increase of permeability near 100°C, is revised as

$$f_3(T)=5.5\left\{\frac{2}{1+\exp[-0.455(T-100)]}-1\right\}+1 \tag{21}$$

which is found by fitting the data used in Bažant and Thonguthai (1978), England and Ross (1970), and Zhukov and Schenchenko (1974) (Fig. 4).

The thermal conductivity of cement, too, depends on the changes of temperature and moisture content significantly. However, the thermal conductivity k is for concrete is much less sensitive to the changes of temperature and moisture than it is for the

hardenened cement paste and concrete. The reason for this difference is that the mineral aggregates, which represent most of the volume of concrete and are usually chemically stable materials (Harmathy 1970), conduct heat no less than the cement paste but do not transfer moisture significantly. In general, the thermal conductivity depends on the volume fraction of aggregate and its type (Bažant and Kaplan 1996; Neville 1997).

Distributed Sources of Water and Heat

When concrete is heated, the chemically bound water becomes free and gets released into the pores. This is reflected in the source term $I_{(w)}$ of the mass conservation condition in Eq. (15). The amount of dehydrated water is obtained experimentally, by weight loss measurements; $w_d(T)=w_h^{105}f_d(T)$, where w_h^{105}=the hydrate water content at 105°C. The values of $f_d(T)$ are interpolated using the experimental data by Harmathy and Allen (1973). At temperatures below 100°C, the phenomenon must be reversed because of further hydration of cement. The increase of the hydrate water content w_h below 100°C may be described as $w_h(t_e)\approx 0.21c[t_e/(\tau_e+t_e)]^{1/3}$, where t_e=equivalent hydration period and $\tau_e=23$ days (see Bažant and Kaplan 1996). Then the distributed water source is $I_{(w)}=\dot{w}_d-\dot{w}_h$.

The distributed heat source term in Eq. (15*b*) is absent when concrete is heated by conduction from the surface. But when concrete is heated by microwaves, the heat source, Eqs. (13) and (14), generated by ohmic heat dissipation within the concrete volume, is significant.

Boundary Conditions

Heat and mass are transferred at the surface to the surrounding environment. Physically accurate modeling of the environment near the surface, which would call for nonlinear hydrodynamics, is not necessary. For heat transfer, it suffices to use Newton's law of cooling (e.g., Chapman 1987) and a similar law for moisture transfer. Thus the boundary conditions simply are

$$\mathbf{n}\cdot\mathbf{J}=B_w(P_S-P_{\text{am}}), \tag{22a}$$

and

$$\mathbf{n}\cdot\mathbf{q}=B_T(T_S-T_{\text{am}}) \tag{22b}$$

where B_w=moisture transfer coefficient and B_T=heat transfer coefficient; $\mathbf{n}$=unit outward normal of the boundary surface; P_{am}=ambient partial pressure of water vapor; T_{am}=ambient temperature; P_S=partial vapor pressure at the surface (i.e., in the capillary pores adjacent to the surface); and T_S=surface temperature. A perfectly sealed (or insulated) surface is a limiting case for $B_w=0$ (or $B_T=0$), and perfect moisture transmission (or heat transmission) is a limiting case for $B_w\to\infty$ (or $B_T\to\infty$). In the case of free convection of air near the surface, B_T is in the range of 5–25 J/m^2 s°C (e.g., Chapman 1987) and $B_w\approx\infty$ (Bažant and Thonguthai 1978).

The heat radiation from the surface, which is the only mechanism of heat loss in a vacuum, is described by Stefan's radiation law

$$\mathbf{n}\cdot\mathbf{q}_r=\gamma\sigma(T_S^4-T_{\text{am}}^4) \tag{23}$$

where $\mathbf{q}_r$=radiation heat flux; σ=Stefan coefficient=5.67×10^{-8} J/m^2 s K^4; and γ=heat emissivity, which varies in the range of 0–1. For a perfectly black surface, $\gamma=1$, while for brick, $\gamma=0.9$ (Jones 2000); because of lack of data, and also because the precise value is not very important, the same emissivity γ as for brick is assumed for concrete. In the absence of vacuum, both the surface heat transfer, Eq. (22), and the radiation, Eq. (23), take place simultaneously. They may be conveniently characterized as

$$\mathbf{n}\cdot\mathbf{q}=B_{\text{eq}}(T_S-T_{\text{am}}) \tag{24}$$

where B_{eq}=equivalent heat transfer coefficient=$B_T+\gamma\sigma(T_S^2+T_{\text{am}}^2)(T_S+T_{\text{am}})$.

Why Not Liquid–Gas Transport Model?

One might wonder why the recent model of Mainguy et al. (2001), or some other multiphase transport model, has not been adopted. In that model, all the mobile water is assumed to consist of liquid (capillary) water and water vapor contained in the gas (air), the pressure gradient of which is regarded as one driving force of transport. From this starting hypothesis, it is deduced that the water transport is controlled by the flow of liquid (capillary) water and involves evaporation and condensation at gas-liquid interfaces. The starting hypothesis, however, ignores the fact that the capillaries in normal hardened cement paste are not continuous (unless the water-cement ratio were abnormally high). While diffusing, the water molecules must pass through nanopores in calcium silicate hydrates only about 1–3 nm wide, which cannot contain liquid water and thus cannot allow its passage. Moreover, since the mean free path of water molecules in a vapor phase is about 80 nm, there is no chance of vapor molecule passage through the tortuous nanopores (they would bounce of pore walls far more often than of each other, and have about equal chance to be reflected forward or backward). Therefore, water molecules can move through such passages only along adsorption layers which fill these pores. Such water transport is controlled not by viscosity of liquid water, but by the lingering times of the adsorbed water molecules on the surface of calcium silicate hydrates (Bažant 1972, 1975). For these reasons, the theory of Mainguy et al. (2001) and numerous other multiphase transport theories are not applicable (the separation of transport of air in Mainguy et al.'s model might be relevant, although this has not been worked out).

References

Ahmed, G. N., and Hurst, J. P. (1997). "Coupled heat and mass transport phenomena in siliceous aggregate concrete slabs subjected to fire." *Fire Mater.*, 21, 161–168.

American Concrete Institute. (ACI). (1994). "Prediction of creep, shrinkage, and temperature effects in concrete structures." *ACI manual of concrete pratice Part 1: Materials and general properties of concrete, ACI 209R-92*, Detroit.

Bažant, Z. P. (1972). "Thermodynamics of interacting continuua with surfaces and creep analysis of concrete structures." *Nucl. Eng. Des.*, 20, 477–505.

Bažant, Z. P. (1975). "Theory of creep and shrinkage in concrete structures: A precis of recent developments." *Mechanics today*, S. Nemat-Nasser, ed., Vol. 2, Pergamon, New York, 1–93.

Bažant, Z. P., and Baweja, S. (1995). "Justification and refinement of Model B3 for concrete creep and shrinkage. 1. Statistics and sensitivity." *Materials and structures*, Vol. 28, RILEM, Paris, 415–430.

Bažant, Z. P., and Baweja, S. (2000). "Creep and shrinkage prediction model for analysis and design of concrete structures: Model B3—short form." *Adam Neville Symposium: Creep and shrinkage—structural design effects*, ACI SP-194, A. Al-Manaseer, ed., American Concrete Institute, Farmington Hills, Mich., 85–100.

Bažant, Z. P., Caner, F. C., Adley, M. D., and Akers, S. A. (2000a). "Fracture rate effect and creep in microplane model for dynamics." *J. Eng. Mech.*, 126(9), 962–970.

Bažant, Z. P., Caner, F. C., Carol, I., Adley, M. D., and Akers, S. A. (2000b). ''Microplane model M4 for concrete I: Formulation with work-conjugate deviatoric stress.'' *J. Eng. Mech.*, 126(9), 944–953.
Bažant, Z. P., and Chern, J. (1987). ''Stress-induced thermal and shrinkage strains in concrete.'' *J. Eng. Mech.*, 113(10), 1493–1511.
Bažant, Z. P., Hauggaard, A. B., Baweja, S., and Ulm, F. (1997). ''Microprestress-solidification theory for concrete creep. I: Aging and drying effects.'' *J. Eng. Mech.*, 123(11), 1188–1194.
Bažant, Z. P., and Kaplan, M. F. (1996). *Concrete at high temperatures*, Longman, London.
Bažant, Z. P., and Najjar, L. J. (1972). ''Nonlinear water diffusion in nonsaturated concrete.'' *Materials and Structures*, Vol. 5, RILEM, Paris, 3–20.
Bažant, Z. P., and Thonguthai, W. (1978). ''Pore pressure and drying of concrete at high temperature.'' *J. Eng. Mech. Div., Am. Soc. Civ. Eng.*, 104(5), 1059–1079.
Bažant, Z. P., and Thonguthai, W. (1979). ''Pore pressure in heated concrete walls: Theoretical prediction.'' *Mag. Concrete. Res.*, 31(107), 67–76.
Bažant, Z. P., and Xi, Y. (1994). ''Drying creep of concrete: constitutive model and new experiments separating its mechanisms.'' *Mater. Struct.*, 27, 3–14.
Bažant, Z. P., and Zi, G. (2001). ''Spatial and temporal scaling of concrete response to extreme environments.'' *Proc., 3rd Int. Conf., Concrete Under Severe Conditions*, N. Banthia, K. Sakai, and O. E. Gjørv, eds., Univ. of British Columbia, Vancouver, BC, 3–10.
Brocca, M., and Bažant, Z. P. (2000). ''Microplane model and metal plasticity.'' *Appl. Mech. Rev.*, 53(10), 265–281.
Caner, F. C., and Bažant, Z. P. (2000). ''Microplane model M4 for concrete II: Algorithm and calibration.'' *J. Eng. Mech.*, 126(9), 954–961.
Chapman, A. J. (1987). *Fundamentals of heat transfer*, Macmillan, New York.
Cheng, D. K. (1983). *Field and wave electromagnetics*, Addison–Wesley, London.
England, G. L., and Ross, A. D. (1970). ''Shrinkage, moisture and pore pressure in heated concrete.'' *Proc., American Concrete Institute Int. Seminar on Concrete for Nuclear Reactors*, West Berlin, Germany, Special Publication No. 34, 883–907.
Felicetti, R., and Gambarova, G. (1998). ''Effects of high temperature on the residual compressive strength of high siliceous concretes.'' *ACI Mater. J.*, 95(4), 395–406.
Gawin, D., Majorana, C. E., and Schrefler, B. A. (1999). ''Numerical analysis of hygrothermal behaviour and damage of concrete at high temperature.'' *Mech. Cohesive-Frict. Mater.*, 4, 37–74.
Hansen, W., and Almudaiheem, J. A. (1987). ''Ultimate drying shrinkage of concrete-Influence of major parameters.'' *ACI Mater. J.*, 84(3), 217–223.
Harmathy, T. Z. (1970). ''Thermal properties of concrete at elevated temperature.'' *J. Mater.*, 5(1), 47–75.
Harmathy, T. Z., and Allen, L. W. (1973). ''Thermal properties of selected masonry unit concrete.'' *ACI J.*, 70(15), 132–142.
Hasted, J. B., and Shah, M. A. (1964). ''Microwave absorption by water in building materials.'' *Br. J. Appl. Phys.*, 15, 825–836.
Hertz, K. (1981). ''Microwave heating for fire material testing of concrete—A theoretical study,'' *Institute of Building Design Rep. No. 144*, Technical Univ. of Denmark, Lyngby, Denmark.
Hertz, K. (1983). ''Microwave heating for fire material testing of concrete—an experimental study.'' *Institute of Building Design, Rep. No. 164*, Technical Univ. of Denmark, Denmark.
Jones, H. R. N. (2000). *Radiation heat transfer*, Oxford Univeristy Press, Oxford.
Lagos, L. E., Li, W., and Ebadian, M. A. (1995). ''Heat transfer within a concrete slab with a finite microwave heating source.'' *Int. J. Heat Mass Transf.*, 38(5), 887–897.
Li, W., Ebadian, M. A., White, T. L., and Grubb, R. G. (1993). ''Heat transfer within a concrete slab applying the microwave decontamination process.'' *J. Heat Transfer*, 115, 42–50.
Mainguy, M., Coussy, O., and Baroghel-Bouny, V. (2001). ''Role of air pressure in drying of weakly permeable materials.'' *J. Eng. Mech.*, 127(6), 582–592.
Meredith, R. J. (1998). *Engineer's handbook of industrial microwave heating*, The Institution of Electrical Engineers, London.
Metaxas, R. C., and Meredith, R. J. (1983). *Industrial microwave heating*, IEEE Power Engineering Series 4, Peter Peregrinus Ltd., Exeter, England.
Moukwa, M., Brodwin, M., Christo, S., Chang, J., and Shah, S. P. (1991). ''The influence of the hydration process upon microwave properties of cements.'' *Cem. Concr. Res.*, 21, 863–872.
Neville, A. M. (1997). *Properties of concrete*, 4th Ed, Wiley, New York.
Shah, M. A., Hasted, J. B., and Moore, L. (1965). ''Microwave absorption by water in building materials: Aerated concrete.'' *Br. J. Appl. Phys.*, 16, 1747–1754.
Spalding, B. (2000). ''Volatility and extractability of Strontium-85, Cesium-134, Cobalt-57, and Uranium after heating hardened portland cement paste.'' *Environ. Sci. Technol.*, 34, 5051–5058.
Taoukis, P., Davis, E. A., Davis, H. T., Gordon, J., and Talmon, Y. (1987). ''Mathematical modeling of microwave thawing by the modified isotherm migration method.'' *J. Food. Sci.*, 52(2), 455–463.
Thuéry, J. (1992). *Microwaves: industrial, scientific, and medical applications*, Artech House, Boston, 104.
Ulm, F.-J., Coussy, O., and Bažant, Z. P. (1999). ''The ''chunnel'' fire I: chemoplastic softening in rapidly heated concrete.'' *J. Eng. Mech.*, 125(3), 272–282.
Vodák, F., Černý, R., Drchalová, J., Hošková, Š., Kapičková, O., Michalko, O., Semerák, P., and Toman, J. (1997). ''Thermophysical properties of concrete for nuclear-safety related structures.'' *Cem. Concr. Res.*, 27(3), 415–426.
von Hippel, A. R. (1954). *Dielectric materials and applications*, MIT Press, Cambridge, Mass.
Wace, P. F., Harker, A. H., and Hills, D. L. (1989). ''Removal of concrete layers from biological shield by microwaves.'' *Rep. No. EUR 12185*, Nuclear Science and Technology, Commission of the European Communities, Brussels, Belgium.
Wait, J. R. (1985). *Electromagnetic wave theory*, Harper & Row, New York.
Watson, A. (1968a). ''Curing of concrete.'' *Microwave power engineering*, E. C. Okress, ed., Vol. 2, Academic, New York.
Watson, A. (1968b). ''Breaking of concrete.'' *Microwave power engineering*, E. C. Okress, ed., Vol. 2, Acdemic, New York.
Wei, C. K., Davis, H. T., Davis, E. A., and Gordon, J. (1985). ''Heat and mass transfer in water-laden sandstone: microwave heating.'' *AIChE J.*, 31(5), 842–848.
White, T. L., Foster, D., Jr., Wilson, C. T., and Schaich, C. R. (1995). ''Phase II microwave concrete decontamination results.'' *ORNL Rep. No. DE-AC05-84OR21400*, Oak Ridge National Laboratory, Oak Ridge, Tenn.
Zhukov, V. V., and Schenchenko, V. I. (1974). ''Investigation of causes of possible spalling and failure of heat-resistant concretes at drying, first heating and cooling.'' *Zharostoikie betony (Heat-resistant concretes)*, K. D. Nekrasov, ed., Stroizdat, Moscow, 32–45.
Zi, G., and Bažant, Z. P. (2001). ''Continuous relaxation spectrum for concrete creep and its incorporation into microplane model M4.'' *J. Eng. Mech.*, 128(12), 1331–1336.
Zi, G., and Bažant, Z. P. (2003). ''Decontamination of radionuclides from concrete by microwave heating. II: Computations.'' *J. Eng. Mech.*, 129(7), 785–792.